

Rb_2CrCl_4 : studies of a two-dimensional classical easy-plane Heisenberg model with in-plane symmetry breaking

This article has been downloaded from IOPscience. Please scroll down to see the full text article.

1989 J. Phys.: Condens. Matter 1 4387

(<http://iopscience.iop.org/0953-8984/1/27/011>)

View [the table of contents for this issue](#), or go to the [journal homepage](#) for more

Download details:

IP Address: 171.66.16.93

The article was downloaded on 10/05/2010 at 18:25

Please note that [terms and conditions apply](#).

Rb₂CrCl₄: studies of a two-dimensional classical easy-plane Heisenberg model with in-plane symmetry breaking

M E Gouvea^{†‡}, G M Wysin[†], A R Bishop[†] and F G Mertens[§]

[†] Los Alamos National Laboratory, Los Alamos, NM 87545, USA

[§] Physics Institute, University of Bayreuth, D-8580 Bayreuth, Federal Republic of Germany

Received 3 October 1988, in final form 19 December 1988

Abstract. We present numerical simulation studies on the two-dimensional easy-plane classical ferromagnetic Heisenberg model with fourfold in-plane symmetry breaking. Continuum limit equations of motion are obtained and some non-linear particular solutions are discussed. Our simulation data are compared with experimental data obtained for Rb₂CrCl₄. We find evidence for two transition temperatures in this model.

1. Introduction

In recent years there has been a considerable amount of theoretical work (Regnault and Rossad-Mignod 1987) concentrated on two-dimensional (2D) or quasi-2D physical systems. Magnetic 2D systems are particularly interesting since they allow treatment based on simple model spin Hamiltonians which have successfully described linear spin waves. Several possibilities of ferromagnetic and antiferromagnetic isotropic or anisotropic exchange interactions and, also, in-plane symmetry breaking can be analytically or numerically studied. Depending on the particular features of each model there can be, for example, one or more 'phase transitions'. In a classical picture, non-linear domain walls, vortices and spin waves are potentially important elementary excitations for the understanding of these models. For a system with easy-plane symmetry there is a topological transition associated with the unbinding of vortex–anti-vortex pairs (Kosterlitz and Thouless 1973) and an additional in-plane symmetry breaking can lead to a further transition depending on the degree of symmetry breaking (Jose *et al* 1977).

Improvements in materials preparation have made available a considerable number of materials that can be classified as quasi-2D magnets. The primary characteristic of such materials is that the inter-planar interaction is much smaller than the intra-planar one so that they behave predominantly two-dimensionally, even in the vicinity of T_c if the three-dimensional (3D) fluctuations are still weak enough to be outside the 3D critical regime (Regnault and Rossad-Mignod 1987).

Rubidium chromous chloride (Rb₂CrCl₄) is one of these layered-type magnets; the nearest-neighbour (NN) inter-planar interaction is about 10^{-4} the NN intra-planar

[‡] Permanent address: Universidade Federal de Minas Gerais, CP702, Belo Horizonte, MG, Brazil.

interaction (Hutchings *et al* 1981). This weak inter-planar coupling is responsible for a 3D ordering at $T_c = 52.2$ K. Several researchers (Fair *et al* 1978, Lindgard *et al* 1980, Hutchings *et al* 1981, 1986, Cornelius *et al* 1986, Kleemann *et al* 1986) have studied the properties of this compound experimentally and, by now, it is well established that the dominant interaction is a ferromagnetic exchange between the NNS in the planes and that single-ion terms restrict the spins' movement to these planes (i.e. easy-plane anisotropy). In terms of these properties, Rb_2CrCl_4 is somewhat similar to K_2CuF_4 , another quasi-2D magnetic material which has been extensively studied (Funahashi *et al* 1976, Moussa and Villain 1977, Hirakawa and Ubukoschi 1981, Hirakawa *et al* 1982). There are, however, important differences between these two compounds. The Cu^{2+} ion in K_2CuF_4 has $S = \frac{1}{2}$ and no in-plane anisotropy is expected in the Hamiltonian. The Cr^{2+} in Rb_2CrCl_4 has a larger spin, $S = 2$, and is thus expected to behave more classically; moreover, it is subject to single-ion anisotropy effects which tend to align spins along the [110] and symmetry-related directions. Although K_2CuF_4 cannot be classified as a true 2D XY magnet, because the interaction is dominantly of Heisenberg type, magnetic measurements and neutron scattering studies have suggested that the transition has a Kosterlitz–Thouless (κT) character, reflecting some easy-plane anisotropy. Observed critical parameters including the inverse correlation length κ and the critical exponent η can be fitted to κT theory with reasonable success. The experimental results are consistent with vortex theory (Hikami and Tsuneto 1980) and with Monte Carlo (MC) simulations (Kawabata and Bishop 1986a) which have shown that the transition temperature $T_{\kappa\text{T}}$ is weakly dependent on the easy-plane anisotropy, except when very close to the Heisenberg model (those studies have not considered an in-plane anisotropy). Similar attempts to identify a κT transition have been made in Rb_2CrCl_4 but a definite conclusion has not been achieved and it is interesting to understand the extent to which the in-plane anisotropy is responsible for the observed discrepancies.

At this point, it is useful to give a brief summary of some of the experimental results obtained for Rb_2CrCl_4 . Inelastic neutron scattering techniques have been used to investigate the low-wavevector spin waves at several temperatures below T_c . Sharp spin waves are observed at all q (Hutchings *et al* (1981, 1986), and references cited therein) with a gap at $q = 0$ due to the in-plane anisotropy. The low-wavevector spin waves renormalise anomalously as the temperature increases towards T_c . Similar renormalisation effects were observed in K_2CuF_4 and have been attributed to 2D XY behaviour (Hirakawa *et al* 1983) which leads to a universal jump in the stiffness constant at $T_{\kappa\text{T}}$ (Nelson and Kosterlitz 1979). However, concerning Rb_2CrCl_4 , it is not yet clear what is the cause of this anomalous renormalisation. Extensive magnetisation studies (Cornelius *et al* 1986) reveal than an isothermal critical behaviour as $M \propto H^{1/\delta}$ (M is the magnetisation and H is the applied field), at low temperatures, leads to a temperature dependence for the δ exponent, another characteristic behaviour predicted by the κT theory. Associating $T_{\kappa\text{T}}$ with the temperature at which $\delta = 15$ (Kosterlitz 1974), a $T_{\kappa\text{T}}$ value of 45.5 K was obtained. However, above T_c the susceptibility can be fitted equally well to a κT theory or to a conventional power-law behaviour and, as stated before, the final results do not permit us to identify unambiguously the true nature of the critical behaviour of Rb_2CrCl_4 .

Our aim in this work is to provide some additional information on dynamics for this particular class of easy-plane ferromagnets with in-plane symmetry breaking. Some MC studies for 2D easy-plane Heisenberg models with Ising and sixfold in-plane symmetry breaking have been performed by Kawabata and Bishop (1986b) but only static thermodynamic properties were studied. On the basis of a simplified model Hamiltonian

proposed by Hutchings *et al* (1981), Kawabata and Bishop considered the Ising in-plane symmetry breaking as appropriate for describing Rb_2CrCl_4 . We shall discuss the relevance of considering the full Hamiltonian (§2). A fourfold symmetry breaking (denoted by $p = 4$), as appropriate to Rb_2CrCl_4 , is particularly interesting since we know from the work of Jose *et al* (1977) that $p = 4$ corresponds to a kind of ‘border-line’ in the sense that systems with $p < 4$ are *not* expected to show a KT transition while systems with $p > 4$ are expected to show two transitions, one of which can be related to a KT transition, and the other to domain ordering. However, those theoretical results were obtained for the planar model and could be modified when out-of-plane spin components are included. Here we have investigated the $p = 4$ case with numerical simulations using a combined MC–molecular dynamics (MC–MD) approach. A (microcanonical) MD integration of equations of motion was performed using initial configurations generated by a MC simulation. The total space–time Fourier transform of the correlation function $S(\mathbf{q}, \omega)$ includes the effect of all excitations and their interactions. Since there are no 3D effects, we have the advantage of isolating purely 2D information. Unfortunately, at this time there is *no* available theory which includes domain walls, vortices, spin waves and interactions between them to which we can compare our numerical experiments. We believe that all these excitations must be considered in order to understand the dynamical aspects related to this system. Nevertheless, the analysis of our simulation data provides useful information, including the existence of two transition temperatures for Rb_2CrCl_4 .

The paper is organised as follows: in § 2, we discuss the model Hamiltonian to be used in our studies Rb_2CrCl_4 including improvements to previous models so as to accommodate large-amplitude (non-linear) excitations; § 3 contains the equations of motion obtained in the context of a continuum theory. Some particular solutions to these equations are also discussed. We present our simulation data and analysis in § 4 and the final conclusions are given in § 5.

2. Model Hamiltonian for Rb_2CrCl_4

It has been established that the magnetic ions in Rb_2CrCl_4 lie in planar square arrays and are coupled via Cl ions situated between them but displaced from the middle of the Cr^{2+} positions (De Lang *et al* 1977, Day *et al* 1979). This distortion causes alternate atoms to have an easy axis in the x direction and y direction, respectively. The previously proposed spin Hamiltonian is

$$H = -J \sum_{ij} \mathbf{S}_i \cdot \mathbf{S}_j - G \sum_i [(S_{1i}^x)^2 + (S_{2i}^y)^2] + D \sum_i (S_i^z)^2. \quad (2.1)$$

The parameters involved have been measured from linear spin-wave dispersion data (Hutchings *et al* 1981). $J = 15.12\text{K}$ is the NN ferromagnetic exchange constant, $G = 3.14\text{K}$ is the staggered single-ion anisotropy constant creating two sublattices 1 and 2, and $D = -0.14\text{K}$ is the planar anisotropy constant. Despite the negative value of D , we still have planar behaviour assured by the high value taken by G .

It has been found (Hutchings *et al* 1981) that the *linear* spin-wave dispersion of Rb_2CrCl_4 is also well described by the following simple model Hamiltonian:

$$\tilde{H} = -J \sum_{ij} \mathbf{S}_i \cdot \mathbf{S}_j + \tilde{D} \sum_i (S_i^z)^2 - \tilde{G} \sum_i (S_i^d)^2 \quad (2.2)$$

where d is along [110] and

$$\begin{aligned}
\tilde{J} &= J \cos 2\alpha \\
\tilde{G} &= G \sin 2\alpha \\
\tilde{D} &= D + (G/2)(1 - \sin 2\alpha)
\end{aligned}
\tag{2.3}$$

$\alpha = G/8J$ corresponds to the canting angle and can be determined by minimising the classical internal energy. Hamiltonian (2.2) is an approximation to (2.1) obtained through a rotation around the z axis and by neglecting the canted two-sublattice structure.

It is important to emphasise that Hamiltonians (2.1) and (2.2) correspond to different in-plane symmetry breaking, which becomes important for *non-linear* effects; we have a fourfold in-plane symmetry from equation (2.1) while equation (2.2) describes a twofold or Ising-like symmetry. It is not surprising that linear spin-wave dispersion data can be described equally well by both Hamiltonians since the spin-wave dispersion is independent of the degree of symmetry breaking (that is, spin waves are perturbations from one of the ground-state configurations). Nevertheless, as was briefly discussed in §1, the degree of the in-plane symmetry can be decisive in determining whether a κT transition is possible in these easy-plane magnets. We can expect that each of these two Hamiltonians supports different non-linear dynamical features. We can note that simply rotating the (x, y) coordinate system by 45° and *retaining* the two-sublattice model leads to a Hamiltonian exactly equivalent to (2.1):

$$H = -J \sum_{ij} \mathbf{S}_i \cdot \mathbf{S}_j + (D + \frac{1}{2}G) \sum_i (S_i^z)^2 - G \sum_i S_{i1}^{x'} S_{i1}^{y'} + G \sum_i S_{i2}^{x'} S_{i2}^{y'}.
\tag{2.4}$$

The primes indicate the new coordinate system where x' is along $[110]$. The competition between the strong NN exchange and the sublattice-dependent twofold in-plane anisotropies (note that they are oriented at 90° to each other) results in an effective fourfold symmetry, plus a small canting. For an accurate description of large-amplitude non-linear excitations in Rb_2CrCl_4 , such as domain walls, it is essential that we use a model Hamiltonian with the correct ($p = 4$) symmetry. In particular, for domain walls, a $p = 4$ Hamiltonian will support 90° domain walls connecting the degenerate in-plane ground states, and a description by a $p = 2$ Hamiltonian can include only 180° domain walls. Also, the interactions of in-plane vortices with these domain walls will be dependent on the total ‘twist’ of the walls. Since T_{KT} can be expected to be a sizeable fraction of JS^2 , it is likely that domain walls may be easily created near the transition temperature and therefore they can play a part in modifying the transition through their interactions with vortices. As a result of this, we expect that an accurate description of a possible symmetry-modified κT transition Rb_2CrCl_4 will require a model which correctly describes the domain walls and their effect on the vortices (and vice versa). For this reason, we have used Hamiltonian (2.1) in our MC–MD simulation studies for Rb_2CrCl_4 .

3. Continuum theory for Rb_2CrCl_4

The spin components can be described by four angular variables since we have two sublattices. Adopting a procedure similar to that used by Mikeska (1980) for the anti-ferromagnetic chain, we define

$$\begin{aligned}
S_{n,m} = S \cos[\Theta_{n,m} + (-1)^{n+m} \theta_{n,m}] \cos[\Phi_{n,m} + (-1)^{n+m} \varphi_{n,m}]; \\
\cos[\Theta_{n,m} + (-1)^{n+m} \theta_{n,m}] \sin[\Phi_{n,m} + (-1)^{n+m} \varphi_{n,m}]; \\
\sin[\Theta_{n,m} + (-1)^{n+m} \theta_{n,m}]
\end{aligned}
\tag{3.1}$$

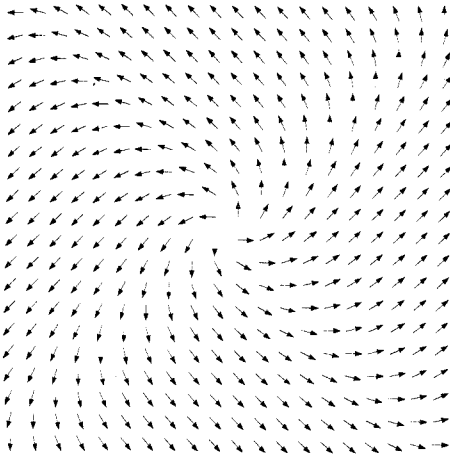


Figure 1. A single vortex given by equation (3.8) (with $x_0 = y_0 = 0, n = g = 1$) plotted on a square lattice.

where (n, m) denotes the spin site in the 2D lattice. For the continuum classical dynamics, we assume that the spin fields $\Theta(\mathbf{r}), \Phi(\mathbf{r}), \theta(\mathbf{r})$ and $\varphi(\mathbf{r})$ ($\mathbf{r} = (r, p)$ in polar coordinates) vary smoothly and also that $\theta(\mathbf{r})$ and $\varphi(\mathbf{r})$ represent small deviations from $\Theta(\mathbf{r})$ and $\Phi(\mathbf{r})$, respectively. Including terms up to second order in spatial derivatives, the continuum equations of motion are

$$(1/JS)\dot{\Theta} = -8\varphi\theta \sin \Theta - 2 \sin \Theta \nabla\Theta \cdot \nabla\Phi + \cos \Theta \nabla^2\Phi + g\theta \sin \Theta \sin 2\Phi - 2g\varphi \cos \Theta \cos 2\Phi \tag{3.2}$$

$$(1/JS)\dot{\Phi} = (8\theta^2 \sin \Theta / \cos^2 \Theta) 8\varphi^2 \sin \Theta - \sin \Theta |\nabla\Phi|^2 - \nabla^2\Theta / \cos \Theta + 2d \sin \Theta + g \sin \Theta (1 - 2\varphi \sin 2\Phi) + g\theta \cos \Theta \cos 2\Phi \tag{3.3}$$

$$(1/JS)\dot{\theta} = -8\varphi \cos \Theta - g \cos \Theta \sin 2\Phi \tag{3.4}$$

$$(1/JS)\dot{\varphi} = 8\theta / \cos \Theta + 2d\theta \cos \Theta + g\theta \cos \Theta + g \sin \Theta \cos 2\Phi \tag{3.5}$$

where $g = G/J$ and $d = D/J$ are taken as small parameters.

It is hard to obtain general solutions to equations (3.2)–(3.5). We shall limit ourselves here to some particular cases. One obvious particular static solution ($\dot{\Theta} = \dot{\Phi} = \dot{\varphi} = \dot{\theta} = 0$) corresponds to

$$\Theta = \theta = 0 \quad \Phi = \pm \pi/4 \tag{3.6a}$$

$$\varphi = (g/8) \sin 2\Phi \tag{3.6b}$$

i.e. planar domains oriented along the $[\pm 1, \pm 1, 0]$ directions. Equation (3.6b) gives the canted structure. Another planar ($\dot{\Theta} = \dot{\theta} = 0$) static solution is given by

$$\nabla^2\Phi = (-g^2/8) \sin 4\Phi \tag{3.7}$$

and equation (3.6b) for φ . Equation (3.7) is a sine-Gordon equation for the Φ variable and the argument of the sine function (4Φ) reflects the fourfold in-plane symmetry breaking. This equation has been studied by Hudak (1982) who obtained a vortex-like solution

$$\varphi = \pm \tan^{-1} \left[\frac{\sinh[g(y - y_0)/2]}{\{\sinh[g(x - x_0)/2]\}^{-1}} - (2n + 1)\pi/2 \right] \tag{3.8}$$

(where n is an integer number) with vorticity ± 1 and which is shown in figure 1. It can

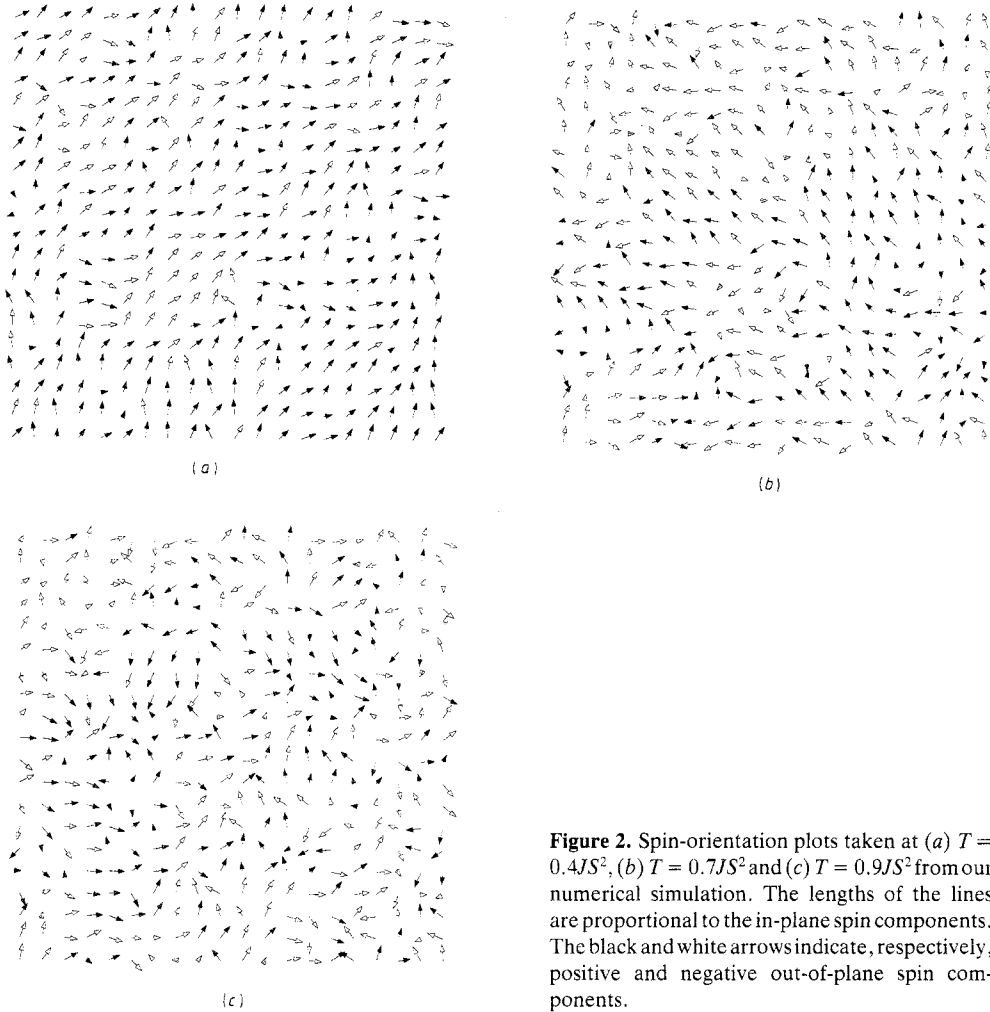


Figure 2. Spin-orientation plots taken at (a) $T = 0.4JS^2$, (b) $T = 0.7JS^2$ and (c) $T = 0.9JS^2$ from our numerical simulation. The lengths of the lines are proportional to the in-plane spin components. The black and white arrows indicate, respectively, positive and negative out-of-plane spin components.

be seen that in the region surrounding the vortex centre (x_0, y_0) the vortex described by (3.8) does not appreciably differ from the usual vortex $\Phi = \pm \tan^{-1}(y/x)$ of the planar model. The difference, however, is strong in the far-field region where the spins form four domains separated from each other by domain walls along $\Phi = (2n + 1)\pi/4$ ($n = 0, +1, \dots$). The energy of this vortex was also estimated by Hudak (1982) and depends linearly on L , the system size. Recall that the energy of a single planar model vortex diverges logarithmically with the size of the system. This logarithmic dependence comes from the fact that, for the planar model, the required 2π rotation of a vortex can be approximately equally divided among all NN pairs; moving along a circle of radius r having the vortex at its centre, the spins are rotated from their neighbours by an angle of about $1/r$ (Einhorn *et al* 1980). The in-plane symmetry of our model does not permit the spins to share equally the 2π rotation and they change their orientation by $\pi/2$ when crossing the domain boundaries. Since the domain boundaries have finite energy per unit length, the energy for a single vortex diverges with L , as found by Hudak, and we should not expect to find vortices, at least at low temperatures. However, vortex-anti-

vortex pairs bound by domain boundaries (strings) have finite energy and can be created, giving rise to a *linear* interaction potential between vortices.

Entropy arguments (Lee and Grinstein 1985, Einhorn *et al* 1980, Tang and Mahanti 1986) can be used to determine the phase diagram. Generally speaking, we could expect a transition temperature T_1 such that at $T > T_1$ the strings connecting vortex–anti-vortex pairs become flexible, and a transition temperature $T_2 = T_{KT}$ due to the unbinding of these pairs. The phase diagram is determined by the relative magnitudes of T_1 and T_2 . Our simulation studies (§ IV) for Hamiltonian (2.1) suggest two transition temperatures, i.e. $T_1 < T_2$.

The particular solutions that we have discussed here are restricted to the X – Y plane. It is interesting to ask whether equations (3.2)–(3.5) also admit static vortex-like solutions with non-zero out-of-plane spin components in the region close to the vortex centre. This kind of solution has been found by Hikami and Tsuneto (1980) for the anisotropic Heisenberg model (without single-ion anisotropy terms). It has been found that the stability of this vortex-like solution depends on the easy-plane anisotropy (Wysin *et al* 1988, Gouvea *et al* 1989). The vortex shape is crucial in determining the out-of-plane correlation function, as discussed in a phenomenological model by Mertens *et al* (1987, 1989).

4. Numerical simulation and analysis

A combined MC–MD method (Kawabata *et al* 1986) was used to determine the equilibrium dynamics, especially for the dynamic structure function $S(\mathbf{q}, \omega)$. Simulations were performed on a 100×100 square lattice for model (2.1), with periodic boundary conditions. In this method, first a MC simulation is performed, producing a set of equilibrium configurations for a desired temperature. These configurations are then used as initial conditions for an energy-conserving MD simulation of the equations of motion. The time integration was performed with a standard fourth-order Runge–Kutta method, with a fixed time step of $0.04(JS)^{-1}$. The spin configuration was sampled at 512 equally spaced times, so that a FFT algorithm could be used for the temporal part of the space–time Fourier transform. To resolve spin-wave peaks adequately for the smallest wavevectors ($q = 2\pi/100a$), it was necessary to integrate to $t \approx 654(JS)^{-1}$. The dynamic structure function $S^{\alpha\alpha}(\mathbf{q}, \omega)$ was then determined from the Fourier transform of the space-and-time-displaced correlation function $\langle S^{\alpha}(\mathbf{0}, 0)S^{\alpha}(\mathbf{r}, t) \rangle$. In particular, we calculated in-plane correlations ($\alpha = x, y$) and out-of-plane correlations ($\alpha = z$). The structure functions resulting from several initial conditions for a given temperature were then averaged together. Typically, we averaged over only three initial conditions, because the calculations required a central processing unit time of about 30 min per initial condition on a CRAY-1S vector machine. We also employed a smoothing algorithm on $S(\mathbf{q}, \omega)$, as did Mertens *et al* (1987, 1989), to reduce the effects of a finite time series and statistical fluctuations.

Figure 2 shows spin-orientation plots taken at several temperatures. From the spin orientations at the lowest temperature, $T = 0.4JS^2$, it can be seen that the spins are largely confined to the X – Y plane. It is possible to identify small domains with the spin polarisation rotated by $\pi/2$ with respect to other domains. As the temperature increases, the out-of-plane spin components increase and, although the plots become increasingly difficult to analyse, we can see that the domains' sizes decrease, consistent with entropy arguments (Einhorn *et al* 1980). It is very difficult to identify vortex-like structures in

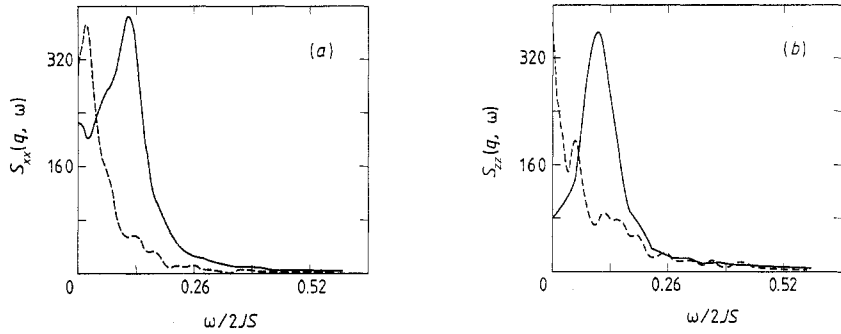


Figure 3. Results from MC-MD simulations of Hamiltonian (2.1) on a 100×100 lattice for $q = (0.10, 0)\pi/a$ for (a) in-plane correlations and (b) out-of-plane correlations. The data taken at two temperatures $T = 0.5JS^2$ (—) and $T = 0.8JS^2$ (---).

these figures; in order to do so, a vorticity algorithm would have to be implemented in the simulation.

The space-time Fourier transforms of the correlation functions $S_{xx}(q, \omega)$ and $S_{zz}(q, \omega)$, for $q = (q, 0)$, are shown in figure 3. A central peak can be seen for all temperatures considered in both in-plane and out-of-plane correlation functions, although it is more intense for $S_{xx}(q, \omega)$ than for $S_{zz}(q, \omega)$ at low temperatures. Experimentally, a central peak has been observed (Hutchings *et al* 1986) near $T_c \approx 0.86JS^2$, the temperature at which 3D ordering occurs. The width Γ_x is seen to vary approximately linearly with q for $T < T_c$ and quadratically for $T > T_c$. This central peak was fitted to a product of two Lorentzians, one for the ω -dependence and one for the q -dependence. Such a Lorentzian in-plane central peak has been proposed on the basis of a phenomenological theory (Mertens *et al* 1987, 1989) for the anisotropic Heisenberg model as due to a ‘gas’ of unbound vortices. The experimental data also give a non-null Γ_x at $q = 0$ (at $T = T_c > T_{KT}$) as predicted by that phenomenology.

The q -dependence of Γ_x for $T = 0.8JS^2$ and $T = 0.9JS^2$, as extracted from our simulation data, is shown in figure 4. It is clear that Γ_x shows distinct behaviour for $q < q_c$ ($q_c \propto \xi^{-1}$, where ξ is the correlation length), which is also in agreement with the phenomenological theory: for $q < q_c$, Γ_x varies smoothly with q while, for $q > q_c$, we have, roughly $\Gamma_x \propto q^2$ (for the XY model, the phenomenology predicts Γ_x varying as $\Gamma \propto (\text{constant} + q^2)$ for small q ($q \ll \xi^{-1}$) and as $\Gamma_x \propto q$ for $q \gg \xi^{-1}$). We emphasize that this phenomenological theory does not include an in-plane anisotropy and discrepancies when comparing it with our system can be expected. However, the qualitative agreement mentioned above suggests that scattering within a gas of vortices can be the dominant contribution to the central peak for temperatures above T_{KT} . For temperatures below T_{KT} , where the vortices are bound into pairs, another mechanism is required for the central peak and domain wall fluctuations are good candidates. Unfortunately, at the present time, assumptions such as these cannot be checked because of the lack of an adequate dynamical theory.

The spin-wave spectrum has been evaluated to first order in the Holstein–Primakoff approximation by Elliott *et al* (1980):

$$\omega_q = 2JS[2 \cos 2\alpha + g \sin 2\alpha - \cos 2\alpha (\cos q_x + \cos q_y)]^{1/2} \\ \times [2 \cos 2\alpha + d + (g/2)(1 + \sin 2\alpha) - (\cos q_x + \cos q_y)]^{1/2}. \quad (4.1)$$

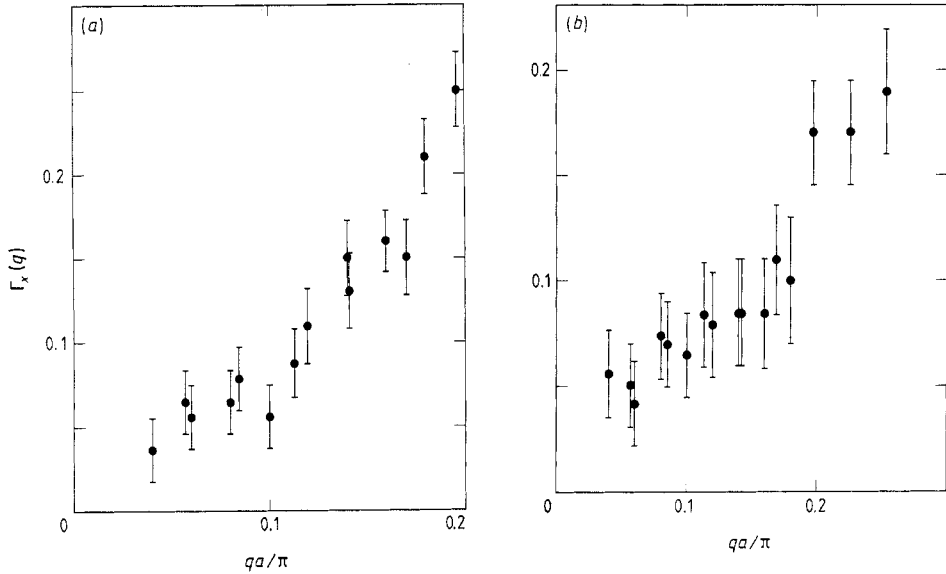


Figure 4. Width Γ_x of central peak in $S_{xx}(q, \omega)$ for (a) $T = 0.8JS^2$ ($q_c \approx 0.1\pi/a$) and (b) $T = 0.9JS^2$ ($q_c \approx 0.2\pi/a$). Data points and error bars result from estimating Γ_x from plots such as figure 3.

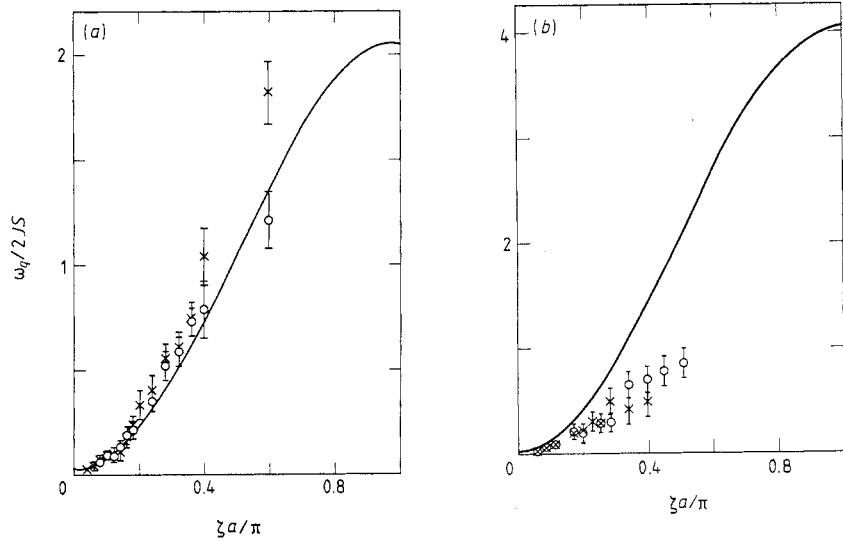


Figure 5. Spin-wave dispersion obtained from the simulation data for wavevectors q along (a) $[\zeta, 0]$ and (b) $[\zeta, \zeta]$ directions at $T = 0.5JS^2$: \times , data taken from $S_{zz}(q, \omega)$ curves; \circ , data taken from $S_{xx}(q, \omega)$ curves; —, equation (4.1).

For finite T , the spectrum has been calculated by Lindgard *et al* (1980) who also included zero-point quantum corrections. Figure 5 shows the spin-wave dispersion obtained from our simulation data for wavevectors along $[\zeta, 0, 0]$ and $[\zeta, \zeta, 0]$ directions at $T = 0.5JS^2$. The full curve corresponds to equation (4.1). It can be seen that the relative renor-

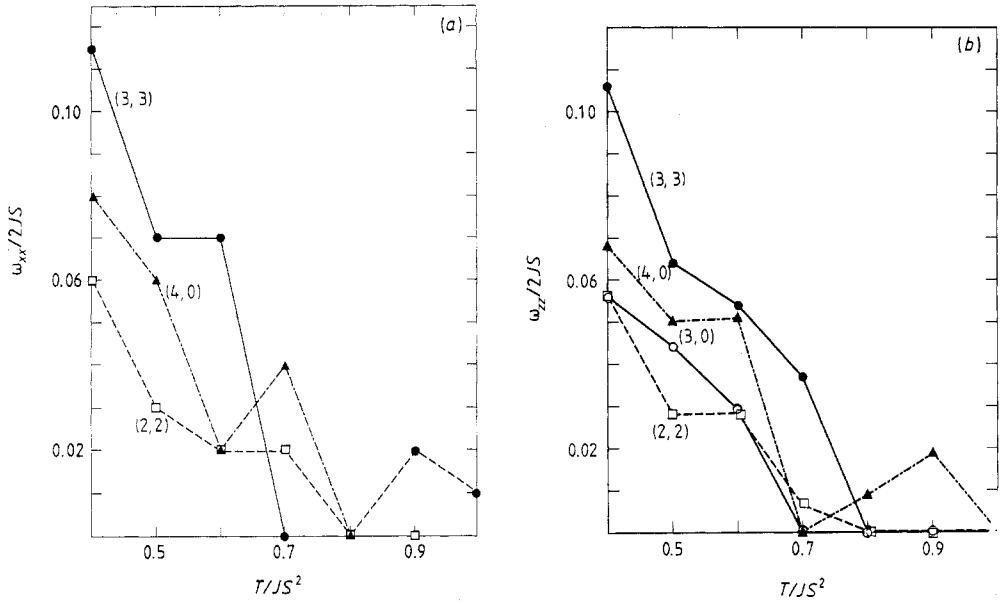


Figure 6. Spin-wave frequencies (from our simulations) as functions of temperature determined from (a) in-plane correlations $S_{xx}(q, \omega)$ and (b) out-of-plane correlations $S_{zz}(q, \omega)$, for various wavevectors given in units of $\pi/50a$.

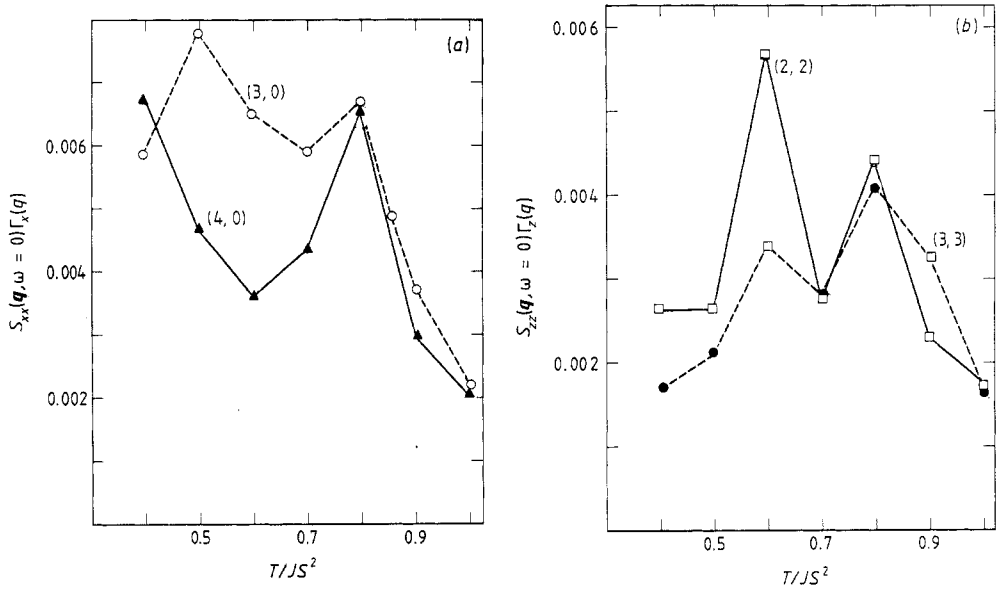


Figure 7. Height $S_{\alpha\alpha}(q, \omega = 0)$ of the central peak ((a) $\alpha = x$ and (b) $\alpha = z$) multiplied by the width $\Gamma_{\alpha\alpha}(q)$ as a function of T , for various wavevectors given in units of $\pi/50a$.

malisation of the mode in the $[\zeta, 0, 0]$ direction is less pronounced than that of the $[\zeta, \zeta, 0]$ mode. A similar observation was made by Fair *et al* (1978) for $[0.15, 0, 0]$ and $[0.1, 0.1, 0]$ modes which have only slightly different wavevectors and energies. This

effect can be due to the in-plane fourfold symmetry. In figure 6 we show how the low-wavevector spin waves renormalise as the temperature increases. As pointed out in § 1, an anomalous renormalisation has been experimentally observed (Hutchings *et al* 1981) and is strongly wavevector dependent, being greatest for the low-wavevector modes. This wavevector dependence is also shown in figure 6.

Figure 7 shows the product of the height $S_{\alpha\alpha}(q, \omega = 0)$ [$\alpha = x, z$] of the central peak and the width $\Gamma_{\alpha}(q)$ as a function of T for low wavevectors. This product is proportional to the intensity of the central peak (the proportionality constant depends on the shape of the peak) which, in the limit $q \rightarrow 0$, can be related to the magnetic susceptibility. These graphs suggest two transition temperatures around $T_1 \approx 0.5JS^2$ and $T_2 \approx 0.8JS^2$: we recall that $T = 0.75JS^2$ has been identified as a possible value for T_{KT} . The procedure adopted here is approximated and simply gives an indication that a transition can occur at each of these temperatures. Simulation studies performed by Kawabata and Bishop (1986a, b) using the simplified Hamiltonian, equation (2.2), also give evidence for two transition temperatures ($T_1 \approx 0.3JS^2$; $T_2 \approx 0.8JS^2$).

5. Conclusion

In this work, we have discussed the effects of in-plane anisotropy fields on the large-amplitude non-linear excitations of 2D easy-plane Heisenberg models. In particular, for Rb_2CrCl_4 , we emphasise the relevance of taking the full Hamiltonian given by equation (2.1) in order to describe domain walls properly and their interaction with vortices.

The comparison between our simulation and experimental data show good qualitative agreement. We were able to observe the spin-wave renormalisation as the temperature increases for both ω_{xx} and ω_{zz} (figure 6) where ω_{xx} and ω_{zz} are spin-wave frequencies determined from the in-plane correlation $S_{xx}(q, \omega)$ and out-of-plane correlation $S_{zz}(q, \omega)$, respectively. The experimental results, taken from neutron scattering experiments, correspond to ω_{xx} renormalisation. Recent simulation studies (Wysin *et al* 1988) on the 2DXY ferromagnetic model also show that both ω_{xx} and ω_{zz} renormalise when $T \rightarrow T_{KT}$, but the softening of ω_{xx} is much stronger than for ω_{zz} . Here the softenings of ω_{zz} and ω_{xx} are comparable and this could be because the interaction is predominantly of the Heisenberg type. On the contrary, the in-plane anisotropy seems to be responsible for the differences observed in the spin-wave dispersion for wavevectors along the $[\zeta, 0, 0]$ and $[\zeta, \zeta, 0]$ directions.

The simulation data also present evidence for two transition temperatures around $T_1 \approx 0.5JS^2$ and $T_2 \approx 0.8JS^2$. Experimentally, it would be very difficult to observe the lower transition T_1 because it is well below the 3D ordering temperature, but the value found for T_2 is in good agreement with the value $T \approx 0.75JS^2$ which has been identified previously as a possible value for T_{KT} for Rb_2CrCl_4 .

Acknowledgments

MEG was supported by CNPq (Conselho Nacional para o Desenvolvimento Científico e Tecnológico, Brazil) and by UFMG (Universidade Federal de Minas Gerais).

References

- Cornelius C A, Day P, Fyne P J, Hutchings M T and Walker P J 1986 *J. Phys. C: Solid State Phys.* **19** 909
- Day P, Hutchings M T, Janke E and Walker P J 1979 *J. Chem. Soc. Chem. Commun.* 711
- De Lang K, Veillet P and Walker P 1977 *J. Phys. C: Solid State Phys.* **10** 4593
- Einhorn M B, Savit R and Ravinovici E 1980 *Nucl. Phys.* **B 170** 16
- Elliott R J, Hengeltraub A, Harrop M C and Ziman T A L 1980 *J. Magn. Magn. Mater.* **15–8** 359
- Fair M J, Hutchings M T, Day P, Ghosh R and Walker P J 1978 *J. Phys. C: Solid State Phys.* **11** L813
- Funahashi A, Moussa F and Steiner M 1976 *Solid State Commun.* **18** 433
- Gouvea M E, Wysin G M, Bishop A R and Mertens F G 1989 *Phys. Rev. B* (June) at press
- Hikami S and Tsuneto T 1980 *Prog. Theor. Phys.* **63** 387
- Hirakawa S and Ubukoschi K 1981 *J. Phys. Soc. Japan* **50** 1909
- Hirakawa K, Yoshizawa H, Axe J D and Shirane G 1983 *J. Phys. Soc. Japan* **52** 4220
- Hirakawa K, Yoshizawa H and Ubukoschi K 1982 *J. Phys. Soc. Japan* **51** 2151
- Hudak O 1982 *Phys. Lett.* **89A** 245
- Hutchings M T, Als-Nielsen J, Lindgard P A and Walker P J 1981 *J. Phys. C: Solid State Phys.* **14** 5327
- Hutchings M T, Day P, Janke E and Pynn R 1986 *J. Magn. Magn. Mater.* **54–7** 673
- Jose J V, Kadanoff L P, Kirkpatrick S and Nelson D R 1977 *Phys. Rev. B* **16** 1217
- Kawabata C and Bishop A R 1986a *Solid State Commun.* **60** 169
- 1986b *Z. Phys.* **B 65** 225
- Kawabata C, Takeuchi M and Bishop A R 1986 *J. Magn. Magn. Mater.* **54–7** 871
- Kleeman W, Otte D, Usadel K D and Brieskorn G 1986 *J. Phys. C: Solid State Phys.* **19** 395
- Kosterlitz J M 1974 *J. Phys. C: Solid State Phys.* **7** 146
- Kosterlitz J M and Thouless D J 1973 *J. Phys. C: Solid State Phys.* **6** 1181
- Lee D H and Grinstein G 1985 *Phys. Rev. Lett.* **55** 541
- Lindgard P A, Als-Nielsen J and Hutchings M T 1980 *J. Magn. Magn. Mater.* **15–8** 343
- Mertens F G, Bishop A R, Wysin G M and Kawabata C 1987 *Phys. Rev. Lett.* **59** 117
- 1989 *Phys. Rev. B* **39** 591
- Mikeska H J 1980 *J. Phys. C: Solid State Phys.* **13** 2913
- Moussa F and Villain J 1977 *Physica B* **86–8** 696
- Nelson D R and Kosterlitz J M 1979 *Phys. Rev. Lett.* **39** 1201
- Regnault L P and Rossad-Mignod J 1987 *Magnetic Properties of Layered Transition Metal Compounds* ed. L J Jongh and R D Willet (Dordrecht: Reidel)
- Tang S and Mahanti S D 1986 *Phys. Rev. B* **33** 3419
- Wysin G M, Gouvea M E, Bishop A R and Mertens F G 1988 *Computer Simulation Studies in Condensed Matter Physics: Recent Developments* ed. D P Landau, K K Mon and H B Schüttler (Berlin: Springer) at press